

Effect of Local Heterogeneity on Dielectric Segmental Relaxation of Poly(vinyl acetate) in Concentrated Solution

Makoto Yada,[†] Masaharu Nakazawa, Osamu Urakawa, Yotaro Morishima, and Keiichiro Adachi*

Department of Macromolecular Science, Graduate School of Science, Osaka University, Toyonaka, Osaka 560-0043, Japan

Received November 23, 1999

ABSTRACT: Dielectric segmental mode relaxation (the α -relaxation) was investigated for toluene solutions of poly(vinyl acetate) (PVAc) and for undiluted PVAc. The relaxation spectra in concentrated solutions were found to be much broad compared with those in the undiluted state and in dilute solution. It was also found that the relaxation spectra broadened with decreasing temperature near the glass transition temperature. For concentrated solutions, the correlation length of local heterogeneity (due to concentration fluctuation) was determined to be 1.0 nm by using small-angle X-ray scattering. On the basis of the assumption that the distribution of relaxation times in logarithmic scale is proportional to the magnitude of the heterogeneity, the temperature dependence of the broadness of loss curves can be explained. Thus, the broad dielectric relaxation spectra in concentrated solutions can be attributed to a local configurational irregularity of the polymer segments and the solvent molecules.

Introduction

Although local segmental motions of flexible polymers in solution or in the bulk state have been studied by various relaxation and scattering techniques, the mechanism of local motions has not been understood fully. Dielectric relaxation spectroscopy is one of those techniques long used.^{1–3} For isolated chains in a dilute solution, various theories^{4–8} predicted that the effects of chain connectivity result in a non-single-exponential autocorrelation function $\varphi(t)$ of the dipoles attached perpendicularly to the chain contour which were classified as type B dipoles by Stockmayer.⁹ It was assumed in refs 4–8 that the test chains are surrounded by a continuous medium. On the other hand, segmental motions in concentrated solutions and in undiluted states are governed by intermolecular cooperative effects as well as intramolecular effects.^{10,11} In the condensed systems, $\varphi(t)$ is represented by a stretched exponential curve (the Kohlrausch–Williams–Watts equation).^{12–14} In terms of the Laplace transform of $\varphi(t)$, it is formally expressed by a sum of exponential functions with various relaxation times. The calculation of the relaxation spectrum for the KWW equation was made by Lindsey and Patterson.¹⁵ Hereafter we call such a relaxation spectrum inherent in the polymer chain dynamics the *intrinsic relaxation spectrum*.

Besides those intrinsic mechanisms, a local heterogeneity also causes a distribution of relaxation times which corresponds to a classical concept of *distribution of relaxation times*. It is expected that such effects are significant in multicomponent systems where a local heterogeneity due to an imperfect miscibility causes a distribution of relaxation times.^{16–22} Shears and Williams observed first that the dielectric relaxation spectra broadened by concentration fluctuation for glass forming liquids.¹⁶ Later Wetton, MacKnight, Fried, and Karasz¹⁷ observed the broadening for blends of poly(2,6-dimethyl-

1,4-phenylene oxide) and poly(styrene-*co*-4-chlorostyrene). Kremer and co-workers¹⁸ reported the influence of concentration fluctuation on the dielectric primary relaxation for a polymer blend composed of poly(cyclohexyl acrylate-*stat*-butyl methacrylate) and polystyrene. They explained the temperature dependence of the broadness of the relaxation spectrum assuming a Gaussian distribution of the local heterogeneity based on the model proposed by Zetsche and Fischer.²⁰ Se et al.²¹ reported the effect of local concentration fluctuation on the dielectric normal and segmental mode relaxations in blends of polyisoprene and polystyrene. Such an effect is expected to become remarkable in temperatures near the phase separation temperature.

Using a photobleaching method, Ediger and co-workers^{23,24} found that even in a single component system (supercooled *o*-terphenyl) a local heterogeneity exists near the glass transition temperature T_g . Ilan and Loring²⁵ simulated chain dynamics using a local vitrification model.

To understand the dielectric relaxation spectra of type B polymers,⁹ it is needed to distinguish the effects of local heterogeneity from the intrinsic relaxation spectrum for the segmental motions. In this article we report the dielectric relaxation spectra in concentrated solution of poly(vinyl acetate) (PVAc) in toluene (Tol), focusing our attention on the effect of local heterogeneity on the dielectric relaxation spectra. To obtain information on the local heterogeneity, we also investigated small-angle X-ray scattering (SAXS) for PVAc solutions.

Experimental Section

Samples. Two samples of poly(vinyl acetate) (PVAc) were used. One coded as PVAc-200 was purchased from Wako Pure Chemical Industries Ltd. (Osaka, Japan) and was purified by reprecipitation from dilute methanol solution in excess amount of water under vigorous stirring. A low molecular weight PVAc coded as PVAc-3 was synthesized by using azobis(isobutyronitrile) in a mixed solvent of benzene and carbon tetrachloride (CCl_4) which worked as a chain transfer reagent. Those PVAc samples were dried under vacuum of 0.01 Torr at 40 °C for 72 h. Weight-average molecular weights M_w of PVAc 200 and

[†] Present address: Dainippon Ink & Chemicals, Sakado, Sakuragi City, 285-8668, Japan.

* To whom correspondence should be addressed.

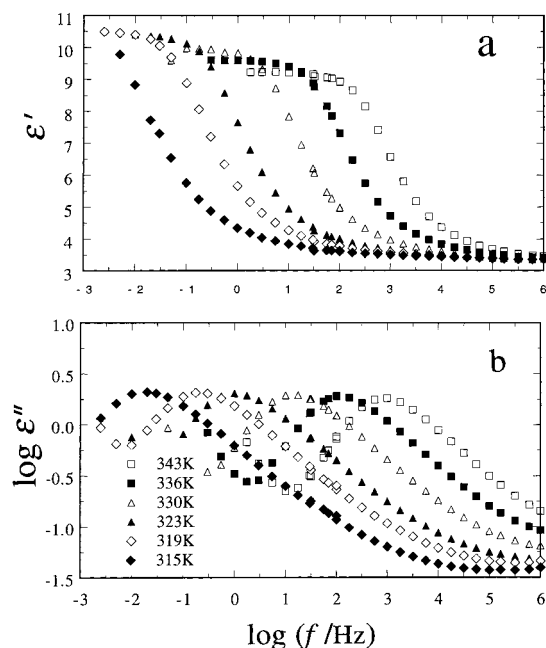


Figure 1. Frequency f dependence of dielectric constant ϵ' (a) and loss factor ϵ'' (b) for undiluted PVAc-200.

PVAc-3 were determined to be 2.0×10^5 and 3000, respectively, by using a size exclusion chromatograph (GPC) equipped with a small-angle light scattering detector (Tosoh LS-8000, Tokyo, Japan). Toluene used as the solvent of sample solutions was of 99.9% pure grade and obtained from Dojin Chemicals (Kumamoto, Japan).

Dielectric Measurements. For dielectric measurements, we used three different apparatuses depending on the frequency range. For measurements in low-frequency range (10^{-3} –10 Hz), we used a homemade apparatus which consisted of a low-frequency generator, a current amplifier (Keithley 427, Cleveland, OH), and sample condenser connected in series. The data of the applied voltage and resulting current were recorded in a personal computer through an AD converter, and the complex dielectric constant ($\epsilon' - i\epsilon''$) was calculated from the amplitude and the phase of the current. An RLC Digibridge (QuadTech 1693, Maynard, MA), an LCR meter (Hewlett-Packard, 4284A, Palo Alto, CA), and a Twin-T bridge (Fujisoku DLB-1101, Tokyo, Japan) were also used for measurements in the range 10 – 10^8 Hz.

Scattering Measurements. Measurements of small-angle X-ray scattering (SAXS) experiments were performed by using BL-10C beam line over a q range from 0.01 to 0.2 \AA^{-1} at the Synchrotron Radiation Facilities in the National Laboratory for High Energy Physics, Tsukuba, Japan.

Results and Discussion

1. Undiluted State and Dilute Solution of PVAc.

Figure 1 shows the double-logarithmic plots of the dielectric constant ϵ' and loss factor ϵ'' for undiluted PVAc-200 against frequency f . As is observed usually,^{1,2} the frequency f_m at which ϵ'' takes the maximum value shifts to lower frequency side with decreasing temperature. The maximum value of ϵ'' slightly increases with decreasing temperature as commonly observed for amorphous polymers. The dielectric relaxation of undiluted PVAc was reported by several authors,^{26,27} and the present results agreed with them. A steep increase of ϵ'' in the low-frequency region is due to ionic conduction due to a trace amount of impurities as observed frequently in dielectric measurements. The slope of the $\log \epsilon''$ vs $\log f$ curve in the high-frequency region is not straight, and the slope decreases with increasing f in

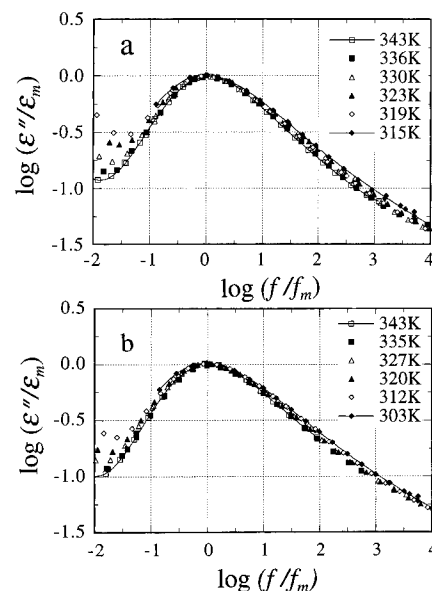


Figure 2. Normalized ϵ'' curves for undiluted PVAc-200 (a) and PVAc-3 (b). Here ϵ_m and f_m denote the maximum value of ϵ'' and the frequency at which ϵ'' becomes maximum.

the range above 100 kHz. This is probably due to the secondary β -relaxation.^{1,2}

The ϵ'' curves of PVAc-3 were observed in a higher frequency range than PVAc-200, reflecting the lower T_g than that of PVAc-200. The shapes of the ϵ' and ϵ'' curves were very similar to those of PVAc-200. Figure 2 shows the normalized ϵ'' curves in which ϵ'' is divided by the maximum value of the loss factor ϵ''_m and frequency f is divided by the loss maximum frequency f_m . It is seen that the ϵ'' curves of PVAc-200 and PVAc-3 broaden with decreasing temperature. However the extent of broadening is small compared with that in concentrated solutions described below. The curves were cast into the Havliriak–Negami equation.²⁸ The parameters α and β of the equation were 0.882 and 0.526, respectively, and are similar to those reported in ref 27. Here α and β are the exponents for the inner and outer brackets of the HN equation, respectively, and $\alpha + \beta = 1$ corresponds to the Debye curve.

We have also carried out dielectric measurements on 5 and 10 wt % solutions of PVAc-200 in toluene. The loss maximum frequencies for 5 and 10% solutions were almost the same. Therefore, 5% solution can be regarded as a dilute solution as far as the relaxation time of the segmental motion is concerned. For 5% solutions of PVAc, Mashimo and Chiba²⁹ reported the ϵ'' curve, which agreed well with the present data. They reported that the ϵ'' curves at various temperatures were superposable and they produced the master curve of ϵ'' . This indicates that the relaxation spectrum for the dilute solution is independent of temperature.

In Figure 3, we compare the shape of the ϵ'' curves among undiluted PVAc-200, PVAc-3, and 5% solution of PVAc-200. In this figure the data points for 5% solution terminates at $\log(f/f_m) = 1.2$. This is due to the limitation of our experimental window ($f < 100 \text{ MHz}$). For the sake of comparison, the ϵ' curve of undiluted PVAc trimer reported by Ikada et al.³⁰ is also plotted. Figure 3 indicates two facts about the effects of the spatial correlation of the dipoles on the relaxation spectrum. First, we note that the shapes of the ϵ'' curves of PVAc-200 and PVAc-3 are almost the same. This indicates that the correlation length of the monomeric

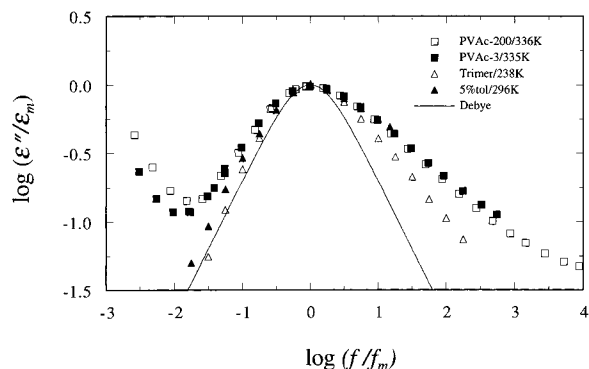


Figure 3. Comparison among the normalized ϵ'' curves of undiluted PVAc-200, undiluted PVAc-3, trimer of PVAc, and 5% solution of PVAc-200. The solid line represents the Debye curve.

dipoles is less than the degree of polymerization of PVAc-3 ($= 35$). But the ϵ'' curve of trimer is narrower than PVAc-3 and PVAc-200, suggesting that the spatial correlation extends more than three monomeric units. Second, we note that the broadness of the ϵ'' curve of the 5% solution is similar to the undiluted PVAc. In the low-frequency side, the ϵ'' curve of the dilute solution is slightly narrower than the undiluted state. We note that the average relaxation times of the bulk and dilute solution differ several orders due to the intermolecular interactions, but the shapes of the ϵ'' curves are similar, indicating that the intermolecular interactions are not reflected strongly on the distribution of relaxation times.

2. Dielectric Relaxation in Concentrated Solution. Representative ϵ' and ϵ''/C curves for 30, 40, and 50 wt % solutions are shown in Figures 4, 5, and 6, respectively, where C represents the concentration in w/v (g/cm^3). In those figures a slight decrease of ϵ' with decreasing frequency is seen. This is due to experimental error. In contrast to the ϵ'' curves of undiluted PVAc, the peak height of these ϵ'' curves decreases slightly with decreasing temperature, and at the same time the ϵ'' curve broadens. This feature was most remarkable in 30 wt % solution. We see that the width of the ϵ'' curve is much broader than those in the undiluted state or dilute solution. Figure 7 compares the normalized ϵ'' curves of the 30% solution. At 193 K, the half-width is 5.0 decades, which is much broader than the half-width of 1.8 decades for 5% solution. It is seen that the ϵ'' curve broadens with decreasing temperature. Similar behavior was observed for 40 and 50 wt % solutions, and the half-widths are listed in Table 1 as a function of T/T_g , where T_g is defined as the temperature at which the loss maximum frequency f_m becomes 0.001. The present results indicate that in concentrated solutions the chain segments experience a range of local environments due to concentration fluctuation as observed by Shears and Williams¹⁶ and Wetton et al.¹⁷

Figure 8 shows the Arrhenius plots of the frequency f_m at which loss becomes maximum for undiluted sample and toluene solutions of PVAc-200. The temperature dependence of f_m can be cast into the Vogel–Fulcher equation:^{31,32}

$$\log f_m = A - B/(T - T_0) \quad (1)$$

where A , B , and T_0 are the adjustable parameters. The parameters A and B are almost independent of concentration, but T_0 depends strongly on concentration as reported previously.³³ We found that slightly different

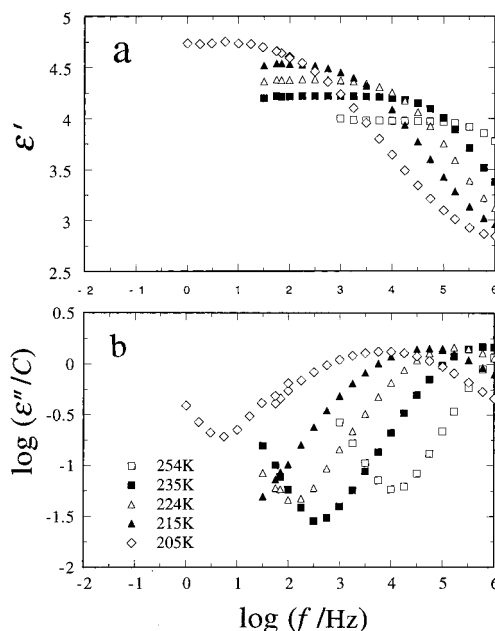


Figure 4. Frequency f dependence of dielectric constant ϵ' (a) and loss factor ϵ'' divided by concentration $C (=0.28 \text{ g}/\text{cm}^3)$ (b) for 30 wt % solution of PVAc-200.

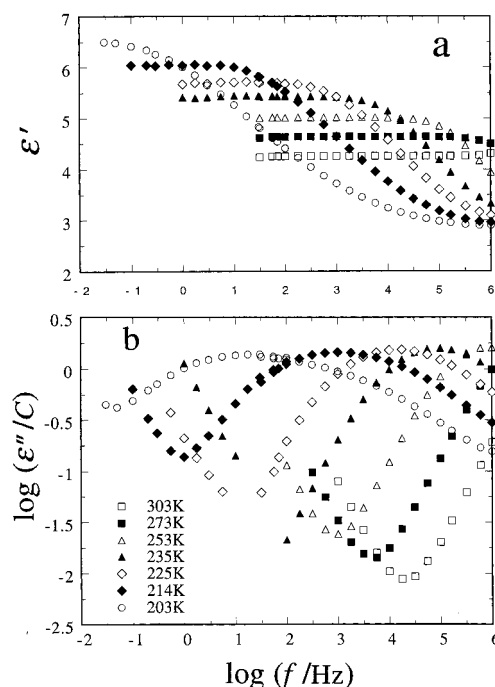


Figure 5. Frequency f dependence of dielectric constant ϵ' (a) and loss factor ϵ'' divided by concentration $C (=0.39 \text{ g}/\text{cm}^3)$ (b) for 40 wt % solution of PVAc-200.

sets of A , B , and T_0 reproduce well the experimental values. If A was fixed to be 12–13, B and T_0 were determined uniquely. Thus, in the present analyses, we attempted to use a common value of $A (=12.1)$. Table 2 lists the values of the parameters thus determined.

The dielectric relaxation strength was determined from the Cole–Cole plots. The effective dipole moment μ per monomeric unit is calculated by the Onsager equation (in cgs units):^{1,34}

$$\Delta\epsilon = \frac{4\pi N\mu^2}{9k_B T} \frac{\epsilon_R(\epsilon_U + 2)^2}{2\epsilon_R + \epsilon_U} \quad (2)$$

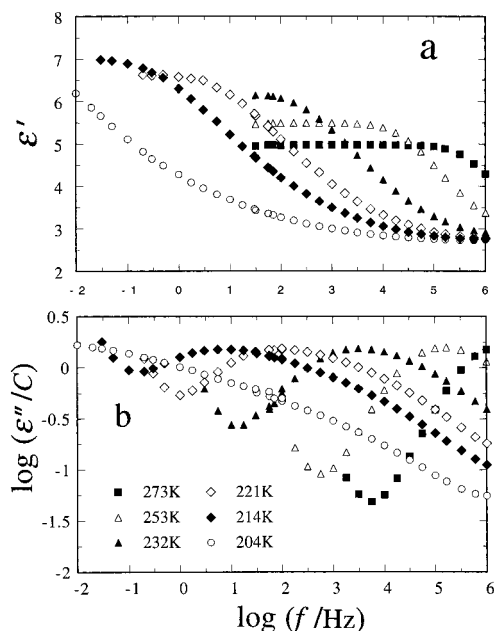


Figure 6. Frequency f dependence of dielectric constant ϵ' (a) and loss factor ϵ'' divided by concentration C ($=0.50$ g/cm³) (b) for 50 wt % solution of PVAc-200.

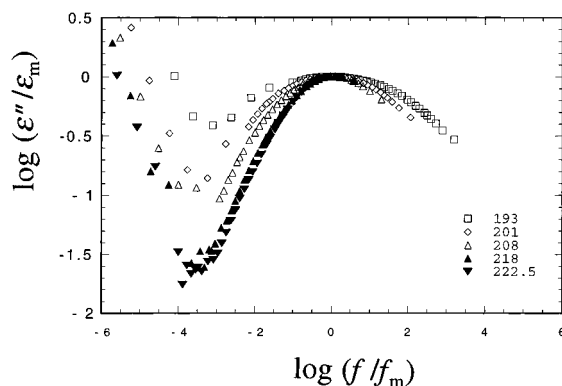


Figure 7. Comparison of the normalized ϵ'' curves at various temperatures for 30 wt % solution of PVAc-200.

Table 1. Half-Width of Dielectric Loss Curve for Bulk and Concentrated Solutions of PVAc^a

wt %	πT_g			
	1.10	1.15	1.20	1.30
30	5.3	4.5	3.8	2.8
40	4.2	3.6	3.1	2.7
50	3.1	2.9	2.7	2.4
100	2.0	1.9	1.9	1.8

^a T_g 's of 30, 40, and 50 wt % solutions and bulk PVAc are 160, 181, 201, and 312 K, respectively.

where N is the number of the monomeric units in unit volume, ϵ_R the relaxed dielectric constant, and ϵ_U the unrelaxed dielectric constant. The values of ϵ_R , ϵ_U , and μ are listed in Table 3. The dipole moment of the ester group μ_0 is reported to be 1.8 ± 0.2 D ($D =$ the Debye unit $= 10^{-18}$ cgs esu), depending on the method of measurement of the dipole moment.^{35,36} The observed values of μ in concentrated solutions are slightly smaller than μ_0 of the free ester group. In the undiluted state, μ is considerably smaller than μ_0 . This can be ascribed to the spatial correlation of the monomeric dipoles due to both the inter- and intramolecular interactions. The Kirkwood correlation factor g is defined by $\mu^2 = g\mu_0^2$, and the values of g are listed in Table 3.³⁷

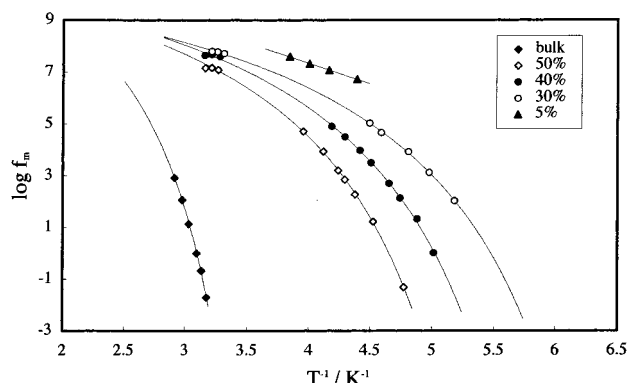


Figure 8. Arrhenius plots of the loss maximum frequency f_m for solutions and bulk PVAc-200.

Table 2. Parameters of Vogel–Flucher Equation for PVAc-200

wt %	C (w/v)	A	B	T_0
30	0.28	12.1	840	104
40	0.39	12.1	755	131
50	0.50	12.1	707	154
100	1.18	12.1	748	260

Table 3. Temperature Dependence of ϵ_R , ϵ_U , μ , and g^a

C (w/v)	T/K	ϵ_R	ϵ_U	μ/D	g^b
0.04	298			1.52	0.71 ^b
	193	5.45	2.70	1.73	0.90
	208	5.05	2.70	1.67	0.84
0.39	223	4.65	2.70	1.59	0.76
	190	7.2	2.80	1.77	0.95
	205	7.0	2.80	1.80	0.98
0.50	222	6.2	2.80	1.71	0.88
	218	8.1	2.9	1.77	0.95
	226	7.5	2.9	1.71	0.88
1.18	243	6.7	2.9	1.62	0.79
	323	10.6	3.4	1.49	0.67
	336	9.7	3.4	1.43	0.62
	343	9.2	3.4	1.39	0.58

^a ϵ_R is the relaxed dielectric constant, ϵ_U is unrelaxed dielectric constant, μ is the dipole moment of the monomeric unit calculated by eq 4, and g is the Kirkwood correlation factor. ^b Determined from the area of the master curve of ϵ'' reported in ref 29.

It is reported that the type B dipoles are not sensitive to the excluded-volume effects,⁹ and hence the g factors demonstrate the intra- and intermolecular correlations of the dipoles. Diaz-Calleja and Riande wrote a nice review on the g factor.³⁸ It was reported that the theoretical g factors due to the intramolecular interactions g_{intra} for various vinyl polymers range mostly from 0.5 to 0.6. Table 3 indicates that the g factor for the bulk PVAc is close to g_{intra} , indicating that the observed g is mostly due to the intramolecular interactions but for solutions the g values are close to unity. This suggests that the solvent molecules may counter the natural intramolecular structural tendency that the dipoles are arranged antiparallel.

We have seen in the previous section that the distribution of relaxation times in concentrated solutions is broader than those in dilute solutions and the undiluted state. However, the present analyses indicate that the monomeric dipoles move without dipolar correlations in concentrated solutions. Therefore, we conclude that the broad distribution of the relaxation spectra in concentrated solutions is not due to the specific interactions among the monomeric units and the solvent molecules.

3. SAXS Measurements. The SAXS profiles at 298, 313, and 333 K for 30 and 40 wt % PVAc/Tol solutions

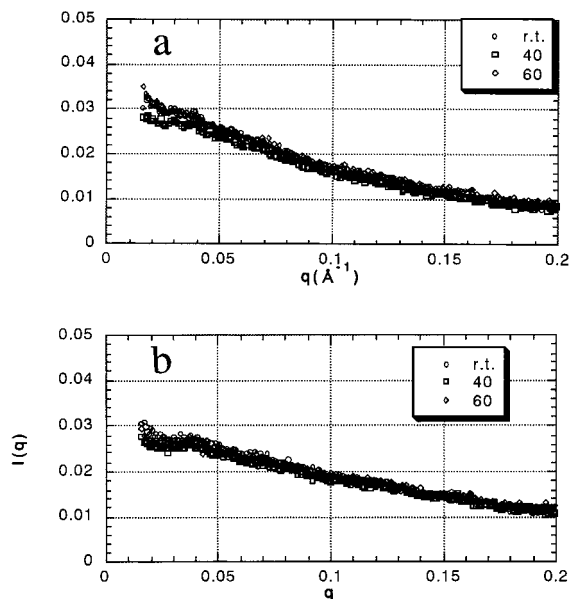


Figure 9. Profiles of small-angle X-ray scattering (SAXS) in 30 wt % (a) and 40 wt % solutions (b) of PVAc-200.

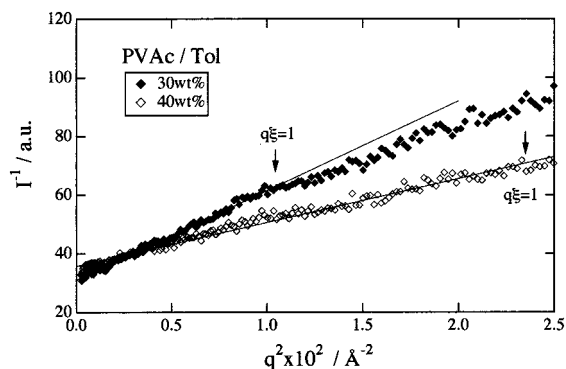


Figure 10. Plots of the inverse of the SAXS intensity against the square of scattering vector q for 30 and 40 wt % solutions of PVAc-200 at 295 K.

are shown in Figure 9. The q range employed here corresponds approximately to the length scale of 0.5–5 nm. To determine the correlation length, we assumed that the scattering profile is given by

$$I(q) = \frac{I(0)}{1 + q^2 \xi^2} \quad (3)$$

where $I(0)$ is the intensity at zero scattering vector and ξ the correlation length. This equation was originally proposed by Ornstein and Zernike³⁹ for liquids near the critical point but is used for the analyses of heterogeneity even at temperatures far from the critical point. The results are shown in Figure 10, and ξ becomes ca. 1.0 nm for 30 wt % solution and 0.65 nm for 40 wt % solution. It is seen in Figure 9 that the intensity is almost independent of temperature, indicating that the values of ξ are almost independent of temperature and therefore ξ depends little on temperature.

4. Distribution of Relaxation Times. 4.1. Relationship between Heterogeneity and Relaxation Spectrum. In Figures 4–6, we see that the ϵ'' curves of concentrated solutions of PVAc broaden significantly with decreasing temperature. On the other hand, undiluted PVAc exhibits less markedly the temperature dependence of the broadness. It has been shown that

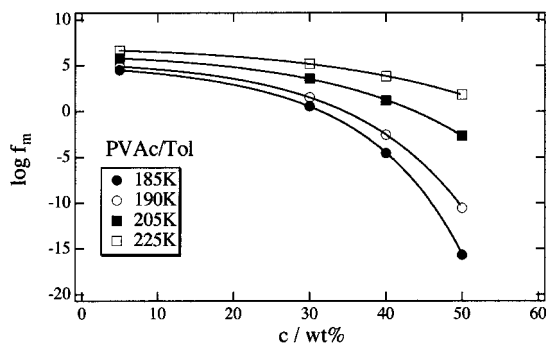


Figure 11. Concentration dependence of the logarithm of loss maximum frequency f_m at various temperatures.

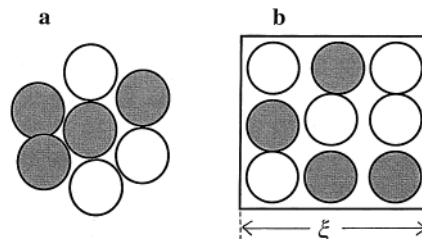


Figure 12. Two models of local heterogeneity in a concentrated polymer solution. The hatched circle represents the polymer segment and the open circle the solvent molecule.

concentrated solutions exhibit a heterogeneity with the correlation length of the order of 1 nm. As is easily expected, if a segment is placed in an environment in which the local concentration ϕ (in unit of number of segments per unit volume) is lower than the macroscopic concentration ϕ_0 , the relaxation time τ is shorter than the average, and vice versa. Here $\phi_0 = N_A C / M_0$ where N_A and M_0 are the Avogadro number and the molecular weight of the monomeric unit, respectively. Thus, a local heterogeneity causes a distribution of τ .

To explain the distribution of dielectric relaxation times of PVAc solutions based on this view, we require information about the amplitude of local concentration fluctuation $\Delta\phi = \phi - \phi_0$ and the $\Delta\phi$ dependence of τ . The broadness of the distribution of relaxation times (in the logarithmic scale) is given by $\Delta\phi$ times $d \log \tau / d\phi$. We assume that the $\Delta\phi$ dependence of τ is the same as the macroscopic concentration (C) dependence of the average relaxation time. From the parameters of the Vogel–Flucher equation^{31,32} given in Table 1, the C dependences of the loss maximum frequency $f_m (=1/2\pi\tau)$ at 185, 190, 205, and 225 K are reproduced as shown in Figure 11. As is seen in this figure, the C dependence of the relaxation time $d \log f_m / dC (\sim -d \log \tau / d\phi)$ becomes strong with decreasing temperature. Since the temperature dependence of $\Delta\phi$ is weak as discussed below, the broadening of the ϵ'' curve with decreasing temperature can be explained from the concentration dependence of τ .

4.2. Microscopic View of Local Heterogeneity. It was shown that the correlation length of the local fluctuation was of the order of 1 nm from SAXS. This length scale is of the order of the size of the monomer. The short-range concentration fluctuation may be understood by considering the probability of the occurrence of configurations of the segments and solvent molecules in a certain space. Two models equally give the same distribution function $P(\phi)$ of local concentration. The first model is shown in Figure 12a in which a test segment is surrounded by n neighboring segments and

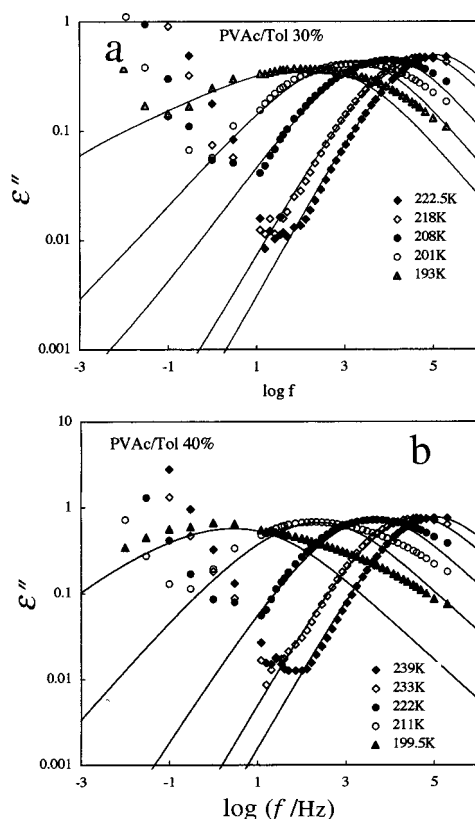


Figure 13. Comparison of the experimental ϵ'' curves and those calculated with eq 10 for 30 wt % solution (a) and that for 40 wt % solution (b).

$z - n$ solvent molecules. The second model is that n segments and $z - n$ segments are confined in a space of the size of the correlation length ξ as shown in Figure 12b. In both models, the local concentration ϕ is proportional to n/z .

To calculate $P(\phi)$, it is needed to assess the interaction energy between the segment and the solvent molecule. The interaction energy U_{p-p} between the polymer segments is taken to be zero. Then U_{p-s} between the polymer and the solvent becomes positive for systems in which the van der Waals force is dominant (regular solutions). Then the probability p that two neighboring lattice points are occupied by the polymer segments may be given by

$$p = \phi_0 / [\phi_0 + (1 - \phi_0) \exp(-U_{p-s}/k_B T)] \quad (4)$$

The solubility parameter δ for PVAc and toluene is reported to be 9.5 and 8.9 cal^{1/2} cm^{3/2}, respectively,⁴⁰ and $U_{p-s}/k_B T$ is calculated to be of the order of 0.02 at $T = 300$ K. Thus, p is close to the average concentration ϕ_0 in the present system.

The probability $P(n)$ for either the model a or b shown in Figure 12 is given by

$$P(n) = p^n (1 - p)^{(z-n)} [z! / n! (z - n)!] \quad (5)$$

Here we note that the temperature dependence of $P(n)$ is weak for the present system as p is almost independent of temperature when T is 200–300 K. Using $\phi = n/z$, we can calculate $P(\phi)$. When z and n are large, $P(\phi)$ reduces to a Gaussian distribution:

$$P(\phi) = (2/\pi z)^{0.5} \exp[-2z(\phi - \phi_0)^2] \quad (6)$$

In the present case, z is expected to be of the order of 10. Numerical calculation of eq 5 indicates that $P(n)$ versus $n/z (= \phi)$ curve for $z = 10$ has a shape close to a Gaussian distribution. Thus, we assume that even for small z and n the local fluctuation of concentration can be approximately given by the Gaussian distribution function as proposed by Zetsche and Fischer:²⁰

$$P(\phi) = A \exp[-(\phi - \phi_0)^2 / 2\sigma] \quad (7)$$

where A and σ ($\cong 1/4z$) are the adjustable constants.

We assume that the distribution function $g(\log \tau/\tau_0)$ of τ is given as a function of ϕ . The inverse of this relation may be written in the form

$$\phi = F(\log \tau/\tau_0) \quad (8)$$

where F denote a certain function. Then from eqs 7 and 8, $g(\log \tau/\tau_0)$ is given by

$$g(\log \tau/\tau_0) = P[F(\log \tau/\tau_0)] \quad (9)$$

where τ_0 is the average relaxation time.

On the basis of this assumption, we attempted to explain the temperature dependence of the distribution of relaxation times of concentrated solutions. It is needed to know the ϵ'' curve for the case in which the local concentration is homogeneous. We assume that the ϵ'' curve exhibiting the intrinsic relaxation spectrum by the Havriliak–Negami equation²⁸ $\Psi(\omega, \tau)$ with the same values of the parameters of the equation as those of the bulk PVAc. Specifically, the parameters used were $\alpha = 0.882$ and $\beta = 0.526$. This assumption was used previously by Zetsche and Fischer.²⁰ Thus, the ϵ'' curves for PVAc/Tol solutions can be written as

$$\epsilon''(\omega) = \int_{-\infty}^{\infty} g(\log \tau/\tau_0) \Psi(\omega, \tau) d \log \tau \quad (10)$$

We also assumed that the relationship between $g(\log \tau)$ and ϕ given by eqs 8 and 9 is similar to the relation between macroscopic τ and C shown in Figure 11. The best fit ϵ'' curves calculated with eq 10 are shown in Figure 13. As is seen in this figure, eq 10 reproduces the experimental loss curve approximately. The parameter σ of eq 7 was 0.05–0.07 for 30 wt % solution. The inverse of σ is of the order of 10 and is consistent with our model proposed above.

Conclusion

We have carried out dielectric measurements on bulk poly(vinyl acetate) (PVAc) and concentrated solutions of PVAc in toluene. The shapes of the ϵ'' curves for undiluted PVAc samples with molecular weight of 200 000 and 3000 are similar, but the ϵ'' curve of the trimer of PVAc is narrower than the high molecular weight samples. This indicates that the correlation of the monomeric dipoles extends more than three repeat units but less than 35 units. The ϵ'' curve for dilute PVAc solutions in toluene is only slightly narrower than that in the bulk state. But for concentrated solutions, we have found that the ϵ'' curves are much broader than the bulk or dilute solution and that the half-widths of the ϵ'' curves increase with decreasing temperature. The dipolar correlation factor does not exhibit remarkable concentration dependence. The correlation length ξ of the heterogeneity is of the order of 1 nm as observed by SAXS. From those results, the broad ϵ'' curves in con-

centrated solutions can be ascribed to local heterogeneity due to concentration fluctuation. The distribution of relaxation times can be explained qualitatively by the amplitude of the heterogeneity times the concentration dependence of the relaxation time. It is demonstrated that the broad ϵ'' curves of concentrated solutions agree with those calculated by assuming a Gaussian distribution of local configurational irregularity. The present results bring up various future problems. It is required to study whether the present results can be seen generally for concentrated solutions of different flexible polymers in good and poor solvents. It is also required to study the local heterogeneity of concentrated solutions by means of different techniques such as NMR.

References and Notes

- (1) McCrum, N. G.; Read, B. E.; Williams, G. *Anelastic and Dielectric Effects in Polymeric Solids*; Wiley: New York, 1967 (reprinted by Dover Publ., New York, 1991).
- (2) *Dielectric Properties of Polymers*; Karasz, F. E., Ed.; Plenum: New York, 1972.
- (3) Adachi, K. In *Dielectric Spectroscopy of Polymeric Materials*; Runt, J. P., Fitzgerald, J. J., Eds.; American Chemical Society: Washington, DC, 1997; Chapter 9.
- (4) Helfand, E. *J. Chem. Phys.* **1971**, *54*, 4651.
- (5) Hall, C. K.; Helfand, E. *J. Chem. Phys.* **1982**, *77*, 3275.
- (6) Valeur, R.; Jarry, J.-P.; Geny, F.; Monnerie, L. *J. Polym. Sci., Polym. Phys. Ed.* **1975**, *13*, 667.
- (7) Bahal, I.; Erman, B. *Macromolecules* **1987**, *20*, 1368.
- (8) Bahal, I.; Erman, B.; Kremer, F.; Fischer, E. W. *Macromolecules* **1992**, *25*, 816.
- (9) Stockmayer, W. H. *Pure Appl. Chem.* **1967**, *15*, 539.
- (10) Adachi, K. *Macromolecules* **1990**, *23*, 1816.
- (11) Matsuoka, S.; Quan, X. *Macromolecules* **1991**, *24*, 2770.
- (12) Williams, G.; Watts, D. C. *Trans. Faraday Soc.* **1970**, *66*, 80.
- (13) Kohlrausch, R. *Prog. Ann. Phys.* **1847**, *12*, 393.
- (14) Ngai, K. L.; Rajagopal, A. K.; Teitler, S. *J. Chem. Phys.* **1988**, *88*, 6088.
- (15) Lindsey, C. P.; Patterson, G. D. *J. Chem. Phys.* **1980**, *73*, 3348.
- (16) Shears, M. S.; Williams, G. *J. Chem. Soc., Faraday Trans.* **1973**, *69*, 608.
- (17) Wetton, A. G.; MacKnight, W. J.; Fried, J. R.; Karasz, F. E. *Macromolecules* **1978**, *11*, 158.
- (18) Katana, G.; Fischer, E. W.; Hack, Th.; Abetz, V.; Kremer, F. *Macromolecules* **1995**, *28*, 2714.
- (19) Alegria, A.; Colmenero, C. M.; Ngai, K. L.; Roland, C. M. *Macromolecules* **1994**, *27*, 4486.
- (20) Zetsche, A.; Fischer, E. W. *Acta Polym.* **1994**, *45*, 168.
- (21) Se, K.; Takayanagi, O.; Adachi, K. *Macromolecules* **1997**, *30*, 4877.
- (22) Runt, J. R. In *Dielectric Spectroscopy of Polymeric Materials*; Runt, J. P., Fitzgerald, J. J., Eds.; American Chemical Society: Washington, DC, 1997; Chapter 10, pp 283–302.
- (23) Ediger, M. D.; Angell, C. A.; Nagel, S. R. *J. Phys. Chem.* **1996**, *100*, 13200.
- (24) Wang, C.-Y.; Ediger, M. D. *J. Phys. Chem.* **1999**, *103*, 4177.
- (25) Ilan, B.; Loring, R. F. *Macromolecules* **1999**, *32*, 949.
- (26) Ishida, Y.; Matsuo, M.; Yamafuji, K. *Kolloid Z.* **1962**, *180*, 108.
- (27) Nozaki, R.; Mashimo, S. *J. Chem. Phys.* **1987**, *87*, 2271.
- (28) Havriliak, S.; Negami, S. *Polymer* **1967**, *8*, 161.
- (29) Mashimo, S.; Chiba, A. *Polym. J.* **1973**, *5*, 41.
- (30) Ikada, E.; Shounaka, K.; Ashida, M. *Polym. J.* **1981**, *13*, 413.
- (31) Vogel, H. *Phys. Z.* **1921**, *22*, 645.
- (32) Fulcher, G. A. *J. Am. Ceram. Soc.* **1925**, *8*, 339.
- (33) Adachi, K.; Hattori, M.; Ishida, Y. *J. Polym. Sci., Polym. Phys. Ed.* **1977**, *15*, 693.
- (34) Onsager, L. *J. Am. Chem. Soc.* **1936**, *58*, 1486.
- (35) Smyth, C. P. *Dielectric Behavior and Structure*; McGraw-Hill: New York, 1955; Chapter 1.
- (36) *Landolt-Bornstein Vol. I, Atom und Molekular Phys. No. 3*; Euchen, A., Hellwege, K. H., Eds.; Springer: Berlin, 1951; p 419.
- (37) Kirkwood, J. G. *J. Chem. Phys.* **1939**, *7*, 911.
- (38) Diaz-Calleza, R.; Riande, E. In *Dielectric Spectroscopy of Polymeric Materials*; Runt, J. P., Fitzgerald, J. J., Eds.; American Chemical Society: Washington, DC, 1997; Chapter 5, pp 139–173.
- (39) Ornstein, L. S.; Zernike, F. *Proc. Acad. Sci. Amsterdam* **1914**, *17*, 793.
- (40) *Polymer Handbook*, 3rd ed.; Brandrup, J., Immergut, E. H., Eds.; John-Wiley: New York, 1989.

MA991973Q